

## Effect of depth increment on damage in incremental sheet forming

Shiori Gondo<sup>1,2,a \*</sup>, Maximilian A. Wollenweber<sup>3,b</sup>, Hamed Dardaei Joghann<sup>2,c</sup>,  
Marlon Hahn<sup>2,d</sup>, Yannis P. Korkolis<sup>2,e</sup> and A. Erman Tekkaya<sup>2,f</sup>

<sup>1</sup>National Institute of Advanced Industrial Science and Technology (AIST), Namiki 1-2-1,  
Tsukuba, Ibaraki, Japan

<sup>2</sup>Institute of Forming Technology and Lightweight Components, TU Dortmund, Baroper Str. 303,  
Dortmund, Germany

<sup>3</sup>Institute for Physical Metallurgy and Materials Physics, RWTH Aachen University, Kopernikus  
Str. 14, Aachen, Germany

<sup>a</sup>shiori-gondo@aist.go.jp, <sup>b</sup>wollenweber@imm.rwth-aachen.de,

<sup>c</sup>hamed.dardaei@iul.tu-dortmund.de, <sup>d</sup>marlon.hahn@iul.tu-dortmund.de,

<sup>e</sup>yannis.korkolis@iul.tu-dortmund.de, <sup>f</sup>erman.tekkaya@iul.tu-dortmund.de

**Keywords:** Incremental Sheet Forming, Dual-Phase Steel, Damage, Void Area Fraction

**Abstract.** Fatigue strength of a part formed by incremental sheet forming (ISF) can potentially be improved by reducing the extent of damage, void area fraction, through control of process parameters. This study aimed to clarify the damage induced by ISF and the effect of process parameters, particularly depth increment during ISF, on the void area fraction. Scanning electron microscopy observation and quantification, trained by a neural network model, found two results: the void area fraction on the tool side was not less than three times smaller than on the rear side of the formed parts, and the fraction decreased with the increase in depth increment.

### Introduction

Incremental sheet forming (ISF) is a process for forming a sheet into a three-dimensional part using a tool that locally and incrementally forms the sheet. This process is typically performed on a computer numerical control (CNC) milling machine. The process parameters can be adjusted locally throughout the process, which is thought to affect the mechanical properties of the formed component [1]. Damage, particularly voids, induced during ISF was focused on among the elements influenced by the process parameters.

Research on bending of DP1180 steel demonstrates a clear influence of the void area fraction in the bent sheet on fatigue strength. Compared to an air-bent sheet, a sheet formed by stress-superposed bending using an elastomer die exhibits lower stress triaxiality at the outer fiber by 0.09 and a smaller void area fraction. As a result, it possesses higher fatigue strength in a multi-step fatigue bending test where the loading force increases incrementally [2]. The stress triaxiality refers to the ratio of hydrostatic stress to the von Mises equivalent stress, and it is well known that large triaxiality promotes damage [3].

Recent research on forging of 16MnCrS5 bulk represents that whether voids grow or close depends on the load path, which refers to the history of hydrostatic stress and deviatoric stress experienced by a material point passing through the forming zone [4]. Research on sheet roll forming of DP800 clarified that stress triaxiality has a greater influence on the void area fraction than strain, even though it is commonly recognized that plastic strain also affects void growth as well as the stress triaxiality does [5]. The findings indicate that when comparing two rolled parts, a conventionally rolled part with  $(\eta, \bar{\epsilon}_p) = (0.58, 0.27)$  and a part rolled using an elastomer die with  $(\eta, \bar{\epsilon}_p) = (0.48, 0.29)$ , the latter exhibits a smaller void area fraction by 33%. The symbols  $\eta$  and  $\bar{\epsilon}_p$  mean the stress triaxiality and equivalent plastic strain. These results suggest that the



histories of hydrostatic stress and deviatoric stresses throughout the entire process, as well as their distribution across the part, potentially vary with the process parameters in ISF. This variation could lead to differences in the void area fractions of the formed part, ultimately improving fatigue strength.

This study aimed to clarify the void area fraction induced in ISF and the effect of process parameters on the void area fraction.

### Experimental Procedures

The sheets used in the experiment were dual-phase steel DP800. Their shape was square, measuring 130 mm on each side and 1.5 mm in thickness. These sheets contained seven complete holes with a diameter of 12.5 mm and two partial holes with a diameter of 20 mm, designed for subsequent fatigue testing as shown in Fig. 1 (a). Table 1 shows the chemical composition of the sheet. The martensite phase fraction was approximately 32% [6]. The tensile strength of the sheets was 834 MPa.

*Table 1 – Chemical composition [mass%] [6]*

C	Si	Mn	Cr	Mo	Cu	Fe
0.15	0.21	1.67	0.73	0.01	0.044	Bal.

Lubricant (Castrol Iloform PN 226) for deep drawing of steels was applied to the tool side surface on the sheet much enough to cover the area where the sheet was going to be deformed. The sheet was formed into a truncated cone shape by ISF using a hemispherical tool tip with a diameter  $d$  of 10 mm, mounted on a conventional 5-axis DMU 50 milling machine manufactured by DMG Mori. Fig. 1 (b) and (c) show the ISF setup and the nominal shape of the formed parts, respectively. The outer edge of the sheet was clamped between a square plate with 20 mm-wide square cavity and a lower support with a width of 15 mm. The tool path alternated between drawing a circle and moving downward by a specified depth increment  $\Delta z$ . The initial circle had a diameter  $d_{\text{ini}}$  of 55 mm, and the depth increments of 0.050 mm, 0.125 mm, and 0.250 mm were used. The final height of the part  $h$  was 15 mm with a wall angle  $\alpha$  of 45 degrees. The movement speed  $v_f$  was set to 1000 mm/min throughout the process.

After forming, white spray was applied to the surface of formed parts to prevent light reflection, and then the parts were then scanned using a three-dimensional scanner based on laser interference fringe analysis (the optical digitizer ATOS Triple Scan from company Carl Zeiss Microscopy GmbH). The middle section's geometry was measured.

The formed parts were cut into rectangles by a cut-off machine using abrasive cut-off wheels so that the plane passing through the center of the sheet would emerge. This plane corresponded to the one used to evaluate the contours of the formed parts. After molding with conductive resins, the parts were polished and etched by a 3% nital solution. Observation through a light microscope revealed that a larger number of voids were present near the corner of the parts. This area was further examined using scanning electron microscopy (SEM), Zeiss Leo 1530 FEG-SEM manufactured by Carl Zeiss Microscopy GmbH. Concretely, a high-resolution panoramic image consisting of several smaller images was taken in the area in order to determine the void area fraction. The individual images were captured in a manner analogous to previous work [7], at an acceleration voltage of 20 kV, a working distance of 10 mm, and a width of 100  $\mu\text{m}$  and 3072 pixels corresponding to a resolution of about 32.6 nm/pixel, with a 15% overlap between neighboring images. The panoramic image was composed of more than 300 images using the microscopy image stitching tool (MIST) plugin in ImageJ [8]. Its width was approximately 1.3 mm and its height coincided with the part thickness. In order to maintain similar imaging conditions and comparability between samples, the brightness and contrast were balanced by equalizing the grey-scale histogram in a post-processing step in MATLAB 2020b. Before the analysis was conducted, the panoramic image was divided into three groups relative to the position

of the image on the sample: the tool side, the center, and the rear side zones. The image was split so that all three regions would remain in roughly similar height which was equal to one-third of the sample thickness. Afterward, the regions were separately analyzed using a damage detection and classification algorithm consisting of two neural networks that have been specifically trained on the analysis of damage sites in DP800 steel as shown in [9,10]. The algorithm located damage sites in the microstructure and classified them. And then, the area void fraction was derived.

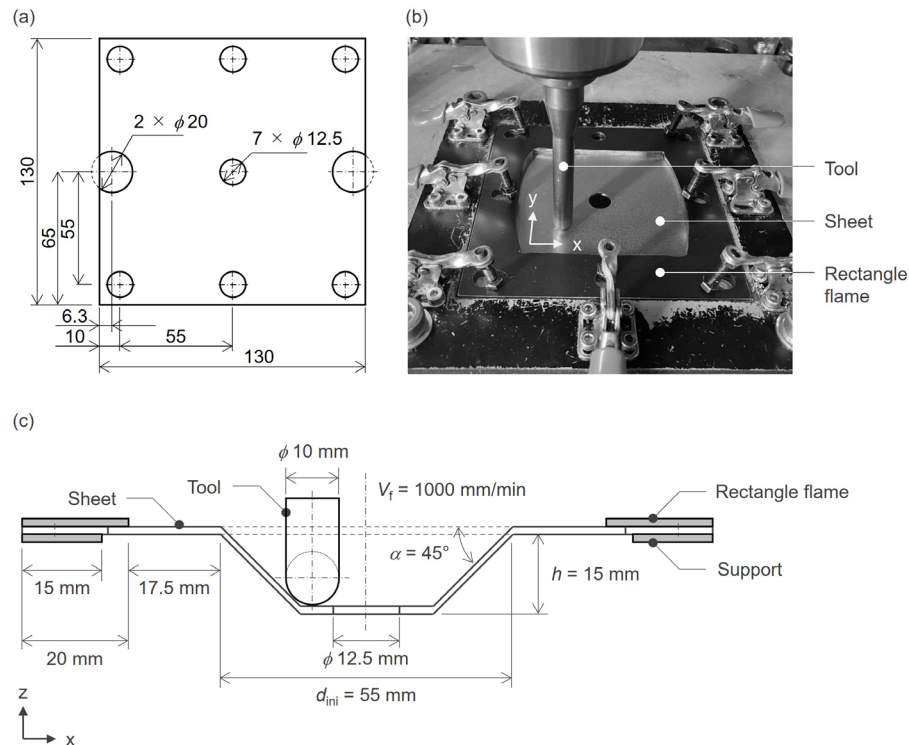


Figure 1 – (a) Dimensions of initial sheet (b) Setup of incremental sheet forming, and (c) nominal geometry of tool path

## Results

Geometrical accuracy of the formed parts. The half of the cross-sectional contour of the formed parts is presented in Fig. 2. The observation plane corresponded to the line marked “A” in Fig. 2 (a). The dashed line represents the nominal contour of the part, as determined by the tool path. There were no data in the range between 0 and 6 mm and 48 mm and 61 mm approximately in Fig 2 (b) because of the holes. All three parts appear to have been influenced by springback. This is evident from the fact that the total height of the part was approximately 1.5 mm smaller than the nominal height, and the wall angle in the area ranging from 25 mm to 30 mm was smaller than the nominal value. Wall angles corresponding to the range from 15 mm to 20 mm in the  $x$  direction in Fig. 2 (b) were  $38.2^\circ$ ,  $37.9^\circ$ , and  $33.5^\circ$  for  $\Delta z$  of 0.050, 0.125, and 0.250 mm, respectively. The wall angle for the part formed under a depth increment of 0.250 mm was smaller than the others by almost  $5^\circ$ .

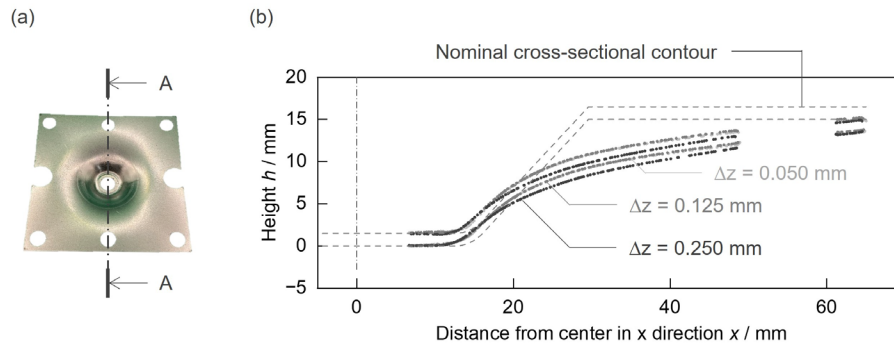


Figure 2 – Cross-sectional contours of half of the formed parts. (a) analysis cross-sectional line and (b) the relationship between distance from center of formed parts and their height.

Effect of depth increment on the void area fraction. As reported in Ref. [11], the following void types were also observed in this study: inclusion, interface decohesion, martensite crack, and notch. Fig. 3 shows the void area fraction of the initial sheet and the parts formed under a depth increment of 0.050 mm, 0.125 mm, and 0.250 mm. Three distinguishable results were found. Firstly, the void area fraction of the initial sheet was extremely small compared to the others, being less than 0.015%. Secondly, the fraction in the rear side zone was approximately 3 times higher than in the tool side zone for a depth increment of 0.050 mm, and 5 times higher for 0.125 mm and 0.250 mm. Thirdly, when comparing the three depth increments, the fraction for a depth increment of 0.050 mm was highest, followed by that for 0.125 mm, and then that for 0.250 mm.

## Discussion

Contours of the formed parts. There is a great difference in shape between every part and the nominal shape at the intersection between the wall and the major base of the truncated cone. In particular, the part formed under the largest depth increment, 0.250 mm, showed the highest variation. These phenomena are consistent with the results obtained using AA1050-O [12]. It is commonly recognized that elastic springback increases as the bending angle increases. The part between the clamped section and the tool position was subjected to bending in this study, as the sheet was clamped between the frame and the support, as shown in Fig. 1 (c). The larger depth increment causes a larger bending angle, which is presumably the main reason for the difference in the wall angle.

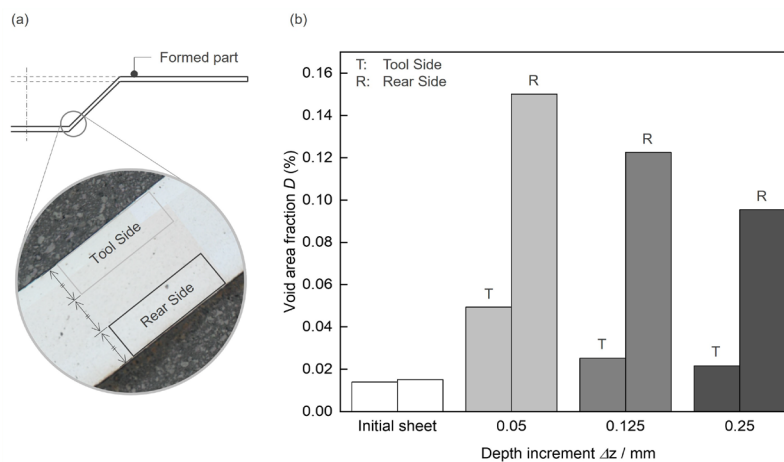


Figure 3 – Void area fraction of the initial sheet and the area near the corner of formed parts

Void area fraction evolution in ISF. The finite element model shows that the part exhibited compressive stress on the tool side in the radial and circumferential directions and tensile stress on the rear side in both directions [13]. The calculation results can be interpreted that the rear side is subjected to positive stress triaxiality and the tool side is subjected to negative triaxiality. This

indicates that the void area fraction on the rear side should be larger than on the tool side. The result shown in Fig. 3 can be explained by this relationship. Meanwhile, the difference in void area fraction caused by the depth increment should be considered based on two reasons. The first is the difference in the stress triaxiality caused by the depth increment while the tool draws one circle. The second is the difference in the load path. Even if the stress triaxiality in one increment for a depth increment of 0.050 mm were to be smaller than that for 0.250 mm, the effect of hydrostatic stress would accumulate. The reason is that the number of times that the tool passes just under the observed area, which has a width of 1.3 mm, is five times larger in the case of a depth increment of 0.050 mm than in the case of 0.250 mm. This point should be discussed based on the finite element model calculation as a future work.

### Summary

This study clarified the damage induced in incremental sheet forming. The following are two key findings.

- 1) The void area fraction on the rear side was three to five times higher than the rear side.
- 2) As the depth increment increased, the void area fraction decreased.

### Acknowledgements

This work is supported by Alexander von Humboldt (AvH) Research Fellowship. Additional support was received by the Deutsche Forschungsgemeinschaft (DFG) in the context of the Collaborative Research Centre CRC/Transregio 188 "Damage Controlled Forming Processes", projects A05 and B02, project no. 278868966.

### References

- [1] F. Maaß, M. Dobecki, M. Hahn, W. Reimers, A. E. Tekkaya, Setting component properties in incremental forming, *Contributed Papers from Materials Science and Technology 2019 (MS&T19)* (2019) 1176-1182. [https://doi.org/10.7449/2019/MST\\_2019\\_1176\\_1182](https://doi.org/10.7449/2019/MST_2019_1176_1182)
- [2] A. E. Tekkaya, N. B. Khalifa, O. Hering, R. Meya, S. Myslicki, F. Walther, Forming-induced damage and its effects on product properties, *CIRP Annals Manuf. Technol.* 66 (2017) 281-284. <http://dx.doi.org/10.1016/j.cirp.2017.04.113>
- [3] T. W. J. de Geus, R. H. J. Peerlings, M. G. D. Geers, Microstructural topology effects on the onset of ductile failure in multi-phase materials – A systematic computational approach, *Int. J. Sold. Struc.* 67-68 (2015) 326-339. <http://dx.doi.org/10.1016/j.ijsolstr.2015.04.035>
- [4] R. Gitschel, A. Schulze, A.E. Tekkaya, Void nucleation, growth and closure in cold forging: an uncoupled modelling approach, *Adv. Ind. Manuf. Eng.* 7 (2023) 100124. <https://doi.org/10.1016/j.aime.2023.100124>
- [5] P. Lennemann, J. Grodotycki, A. E. Tekkaya, Controlling the damage evolution in roll forming of a V-section by elastomer rollers, *Proceedings of the 14th International Conference on the Technology of Plasticity (ICTP2023) - Current Trends in the Technology of Plasticity. ICTP 2023. Lecture Notes in Mechanical Engineering. Springer.* (2024) 266-274. [https://doi.org/10.1007/978-3-031-42093-1\\_26](https://doi.org/10.1007/978-3-031-42093-1_26)
- [6] F. Pütz, F. Shen, M. Könnemann, S. Münstermann, The differences of damage initiation and accumulation of DP steels: a numerical and experimental analysis, *Int. J. Fract.* 226 (2020) 1-15. <https://doi.org/10.1007/s10704-020-00457-z>
- [7] M. A. Wollenweber, S. Medghalchi, L.R. Guimarães, N. Lohrey, C.F. Kusche, U. Kerzel, T. Al-Samman, S. Korte-Kerzel, On the damage behaviour in dual-phase DP800 steel deformed in single and combined strain paths, *Mater. Des.* 231 (2023) 112016. <https://doi.org/10.1016/j.matdes.2023.112016>

- [8] Information on <https://github.com/usnistgov/MIST>
- [9] C. Kusche, T. Reclik, M. Freund, T. Al-Samman, U. Kerzel, S. Korte-Kerzel, P. Pławiak, Large-area, high-resolution characterisation and classification of damage mechanisms in dual-phase steel using deep learning, *PLoS one* 14-5 (2019) e0216493. <https://doi.org/10.1371/journal.pone.0216493>
- [10] S. Medghalchi, C.F. Kusche, E. Karimi, U. Kerzel, S. Korte-Kerzel, Damage analysis in dual-phase steel using deep learning: transfer from uniaxial to biaxial straining conditions by image data augmentation, *JOM* 72-12 (2020) 4420-4430. <https://doi.org/10.1007/s11837-020-04404-0>
- [11] S. Medghalchi, E. Karimi, S. Lee, B. Berkels, U. Kerzel, S. Korte-Kerzel, Three-dimensional characterisation of deformation-induced damage in dual phase steel using deep learning, *Mater. Des.* 232 (2023) 112108. <https://doi.org/10.1016/j.matdes.2023.112108>
- [12] G. Ambrogio, I. Costantino, L. De Napoli, L. Filice, L. Fratini, M. Muzzupappa, Influence of some relevant process parameters on the dimensional accuracy in incremental forming: a numerical and experimental investigation, *J. Mater. Technol.* 153-154 (2004) 501-507. <https://doi.org/10.1016/j.jmatprotec.2004.04.139>
- [13] D. M. Neto, J. M. P. Martins, M. C. Oliveira, L. F. Menezes, J. L. Alves, Evaluation of strain and stress states in the single point incremental forming process, *Int. J. Adv. Manuf. Technol.* 85 (2016) 521-534. <https://doi.org/10.1007/s00170-015-7954-9>